SECOND EUROPEAN CONFERENCE ON EARTHQUAKE ENGINEERING
AND SEISMOLOGY, ISTANBUL AUG. 25-29, 2014

MODELLING OF FRICTION PENDULUM ISOLATORS IN STRUCTURES SUBJECTED TO HORIZONTAL AND VERTICAL GROUND MOTIONS

Pier Paolo DIOTALLEVI[1], Luca LANDI[2] and Gianluca GRAZI[3]

ABSTRACT

This research focuses on the different modelling approaches for the simulation of the seismic response of structures with friction pendulum isolation systems. The behaviour of such systems is strongly affected by several parameters, as for example the friction coefficient and the axial load. The latter has a particular importance in presence of seismic actions characterized by the simultaneous presence of high horizontal and vertical accelerations. In many recent seismic events, as for example L'Aquila (2009) and Emilia (2012) in Italy, the vertical seismic component has been characterized by very high values of acceleration and has played a crucial role in damaging the buildings. To study these aspects, several nonlinear dynamic analyses have been performed considering a two degree of freedom model isolated at the base and subjected to recorded horizontal and vertical ground motions. The response of the isolation systems has been studied through different models, starting by the more simple ones based on constant friction coefficient to the more complex ones based on a friction coefficient varying as a function of sliding velocity and axial force. The analyses have been performed considering a set of ground motions with near field records that present different values of the ratio between the peak vertical and horizontal accelerations. The records have been also applied considering increasing values of intensity, in order to determine the collapse acceleration. The results have allowed to compare the different models and to study the effect of the vertical seismic component on the response of the isolators.

INTRODUCTION

The Friction Pendulum isolation system combines two fundamental mechanisms: the frictional sliding of steel surfaces, which are separated by a Teflon layer, and the pendular motion of the slider on a perfectly spherical surface. Through these mechanisms, the device is able to recenter by itself and can dissipate a large quantity of energy through the sliding on a curved surface. The kinetic energy is partially converted into thermal energy through the overheating of the surfaces in contact and partially in potential energy through the uplift of the structure; the latter pulls back the oscillating mass to its initial position of stable equilibrium, thus providing recentering. The definition of the friction coefficient allows an evaluation of the amount of energy that is dissipated through the isolation system (Constantinou et al.,1990 and 1991). Another important property is that torsional motions of the superstructure are minimized; this result is given by the fact that the horizontal stiffness and the frictional force in each single isolator are directly proportional to the normal force acting on them. In this way, the centre of rigidity of the devices constantly coincides with the centre of mass of the

[1] Professor, Dept. DICAM, University of Bologna, Bologna, pierpaolo.diotallevi@unibo.it
[2] Assistant Professor, Dept. DICAM, University of Bologna, Bologna, luca.landi@unibo.it
[3] Graduate Research Assistant, Dept. DICAM, University of Bologna, Bologna, gianluca.grazi1@gmail.com

structure, compensating the mass eccentricity of the superstructure. There are some problematic issues that are related to the choice of the FPS isolator; its large size, for example, or the influence of vertical movements that are inevitably related to horizontal displacements and that may produce parasitic effects on the structure, thus compromising its correct behaviour (Calvi et al., 2004). High values of the ratio $V/H = PGA_V/PGA_H$ between the peak ground acceleration in the vertical direction (PGA_V) and the corresponding peak in the horizontal direction (PGA_H), which are typical of "near-fault" earthquakes, can cause significant variations in the axial force in reinforced concrete columns, thus introducing adverse phenomena (like brittle collapse in compression or tensile collapse, instability of longitudinal bars, loss of bond between steel and concrete); other effects can be the creation of plastic hinges along the beam span, especially on the higher floors (Diotallevi et al., 2006; Diotallevi and Landi, 2006; Mazza and Vulcano, 2008; Papazoglou and Elnashai, 1996). Moreover, high values of V/H can lead to dangerous tensile stresses on the bearings, causing unexpected mechanisms, which may affect the isolator response with unforeseen breaks or sliding elements coming out of their seat. Moreover, a study of the influence of this component together with bidirectional horizontal seismic action would be necessary in order to consider all three components of the seismic acceleration (Mosqueda et al., 2004). The objective of this study is to evaluate the response of a structure characterized by different functions for the stiffness of the isolator and to consider the effect of the vertical ground motions on the overall behaviour.

HORIZONTAL AND VERTICAL BEHAVIOUR OF THE ISOLATION SYSTEM

The effects of seismic isolation can be studied through a linear elastic system with concentrated masses (Fig.1), which is an extreme simplification of the model in which masses, stiffness and energy dissipation of the superstructure are distributed along the height of the building. The model is characterized by two degrees of freedom, which correspond to the horizontal displacements of the superstructure and of the substructure, indicated as u_s and u_b, while u_g represents the displacement of the ground.

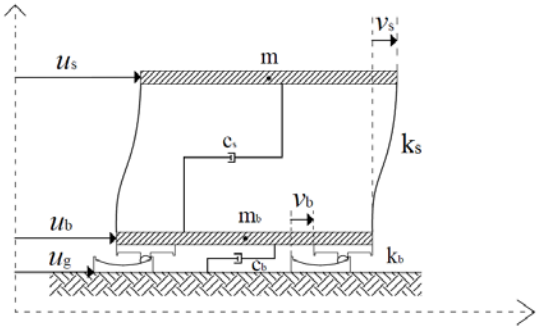

Figure 1. Two degree of freedom isolated system.

The relative displacements are $v_b = u_b - u_g$ and $v_s = u_s - u_b$. The basic equations of motion of the two degree of freedom model are (Kelly and Naeim, 1999):

$$\begin{cases} (m+m_b)\ddot{v}_b + m\ddot{v}_s + c_b\dot{v}_b + k_b v_b = -(m+m_b)\ddot{u}_g \\ m(\ddot{v}_s + \ddot{v}_b) + c_s\dot{v}_s + k_s v_s = -m\ddot{u}_g \end{cases} \quad (1)$$

where m and m_b are the masses of the superstructure and of the substructure respectively; k_s and k_b are the stiffness of the superstructure and of the isolation system respectively; c_s and c_b, are the damping coefficients of the superstructure and of the isolation system respectively. The fundamental equations are integrated step by step with the 4th order Runge Kutta explicit integration method, and the attention is focused on the parameters that are modelled with appropriate non linear functions, such as the isolator stiffness k_b and the isolator damping c_b.

Assuming small deformations, the unidirectional horizontal force-deformation response of the

FPS is given by Eq.(2) (Zayas et al., 1987):

$$F_H = N[\mu\, sign(\dot{v}_b) + v_b / R] \tag{2}$$

where N is the normal force on the isolator (equal to $m+m_b$ in the absence of vertical accelerations), R is the radius of curvature of the spherical surface, v_b is the sliding deformation, $\dot{v}_b$ is the sliding velocity and μ is the friction coefficient at the Teflon-steel interface (Fig. 2).

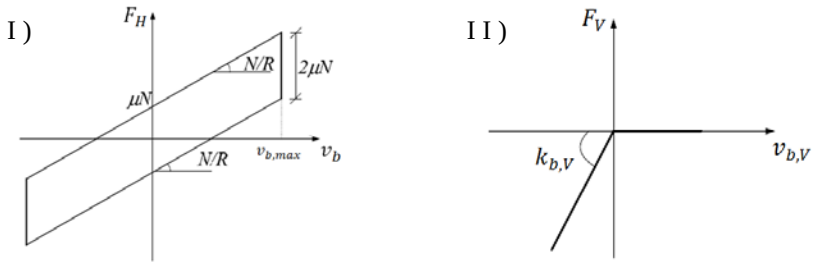

Figure 2. I) Force-deformation diagram of the unidirectional rigid-plastic response of the FPS; II) Force-deformation model of the “Gap” element.

The normal force N, acting on the FPS isolator, affects the horizontal force F_H and consequently the horizontal response of the entire system. An increase in modulus of N causes a large yielding force, which can delay the mobilization of the isolator under dynamic loads, and a high post-elastic stiffness, which can reduce the deformation of the isolator (bilinear behaviour). Besides, μ varies in modulus with N. The conventional FPS isolator does not resist to tensile load. This behaviour corresponds to the response of a "gap" element which is defined by the following relation:

$$F_V = N = \begin{cases} k_{b,V} v_{b,V} + c_v \dot{v}_{b,V} & \text{if} \quad v_{b,V} \le 0 \\ 0 & \text{if} \quad v_{b,V} > 0 \end{cases} \tag{3}$$

where $k_{b,V}$ is the compression stiffness and $v_{b,V}$ is the vertical displacement of the isolator; besides, it is necessary to specify the additional damping coefficient c_V for the vertical degree of freedom. In the vertical direction we can estimate the damping coefficient that is needed to achieve a certain ratio, r, of critical damping (e.g. r = 0.05) from Eq.(4):

$$r = \frac{c_v}{2\sqrt{k_{b,V}(m+m_b)}} \tag{4}$$

The equation of motion in the vertical direction is similar to that for the horizontal direction defined by Eq.(1).

ANALYTICAL MODELS FOR ISOLATOR STIFFNESS AND DAMPING

This section illustrates a brief description of the various models adopted for the schematization of the stiffness and damping parameters of the FPS isolators, starting from the simplest to the most complex.

A) The first considered model is characterized by equivalent parameters for stiffness and damping (the procedure is currently used in the design of the devices). In this model the response is assumed as linear elastic. The stiffness is constant and the energy dissipation per force-displacement cycle is taken into consideration through an equivalent damping:

$$k_b = (m+m_b) g (1/R + \mu / v_{b,\max}) \quad \text{with} \quad \mu = \text{constant} \tag{5}$$

$$\xi_b = \frac{2}{\pi}\frac{\mu}{v_{b,\max}/R + \mu} \tag{6}$$

where $v_{b,\max}$ is the maximum displacement reached by the device.

B) The second model, called Coulomb model (Davis and Mostaghel,1997; Mostaghel, 2004), is characterized by a constant friction and by a non-linear function for the stiffness:

$$k_b(v_b) = (m + m_b)g\left(\frac{1}{R} + \frac{\mu\, sign(\dot{v}_b)}{v_b}\right) \text{ with } \mu = \text{constant} \tag{7}$$

where $sign(\dot{v}_b)$ is the sign function of velocity.

C) The third considered model is more complex, compared to the previous model, since the function of the friction follows the trend given by Eq.(8), obtained from accurate mathematical models developed by Constantinou et al. (1991):

$$\mu(\dot{v}_b) = f_{\max} - (f_{\max} - f_{\min})e^{-a\cdot|\dot{v}_b|} \tag{8}$$

$$k_b(v_b) = (m + m_b)g\left(\frac{1}{R} + \frac{\mu(\dot{v}_b)\, sign(\dot{v}_b)}{v_b}\right) \tag{9}$$

where f_{max} and f_{min} are the values of the friction coefficients corresponding to high and low values of the sliding velocity respectively, and a is a constant that controls the variation of the friction coefficient with velocity. These parameters are evaluated through the linear interpolation of the values provided by Constantinou et al. (1991).

D) In the fourth model the sign function of the velocity is replaced with a continuous function introduced by Bouc and Wen (Wen, 1976) and characterized by the dimensionless hysteretic parameter Z that evolves according to the following differential equation:

$$\dot{Z} = \frac{1}{Y}\left(-\gamma|\dot{v}_b||Z|^{\eta-1}Z - \beta\,\dot{v}_b|Z|^{\eta} + A\dot{v}_b\right) \tag{10}$$

where the parameters of Eq.(10) can be defined as suggested by Constantinou et al. (1991).

E) The fifth model, proposed by the authors, corresponds to the previous model in the horizontal direction. The difference is that it involves also the integration of the equations of motion in the vertical direction, in order to evaluate the normal force vector which will be used as input for the integration of the equations in the horizontal direction. In this way, we can evaluate the new parameters of stiffness and friction, taking into account the variation of the normal force.

$$\mu(\dot{v}_b, N) = f_{\max}(N) - [f_{\max}(N) - f_{\min}(N)]e^{-a(N)|\dot{v}_b|} \tag{11}$$

$$k_b(v_b, N) = N\, g\left(\frac{1}{R} + \frac{\mu(\dot{v}_b, N)\, Z(\dot{v}_b)}{v_b}\right) \tag{12}$$

SELECTED EARTHQUAKE MOTIONS AND STRUCTURES UNDER STUDY

"Near-fault" earthquakes are characterized by long duration impulses in the horizontal direction, which have an increased intensity in the direction normal to the fault line, and by a high frequency motion in the vertical direction. These earthquakes can become critical in base-isolated structures, in particular with Friction Pendulum isolation systems, which are particularly sensitive to traction and uplifting.

For the simulations performed, we have selected nine ground motions characterized by a large acceleration in the horizontal and vertical directions; two of them are records obtained from the recent Italian earthquakes of L'Aquila and Emilia (Table 1). The records have been chosen with the purpose to consider different values of the V/H ratio.

Table 1. Selected ground motions for the analyses.

NAME	*DATE /TIME*	*STATION*	*MAGNITUDE*	PGA_H *[m/s²]*	PGA_V *[m/s²]*	*V/H*
1 ELCE	19/05/1940	El Centro	6.95	3.07	2.01	0.65
2 PACO	09/02/1971	Pacoima Dam	6.61	12.02	6.85	0.57
3 NEWH	17/01/1994	Newhall	6.69	5.79	5.81	1.00
4 SATI	17/01/1994	Saticoy	6.69	1.23	0.51	0.41
5 KJM	16/01/1995	KJMA	6.9	8.07	3.38	0.42
6 COPP	06/04/2009	Coppito	6.3	6.44	4.87	0.76
7 STURN	23/11/1980	Sturno	6.9	3.51	2.55	0.73
8 TOLM	06/05/1976	Tolmezzo	6.5	3.45	3.94	1.14
9 MIRA	20/05/2012	Mirandola	5.9	2.89	8.72	3.02

Table 2. Properties of the Isolation Systems.

N°	**ISOLATOR**	**RADIUS [m]**	**DIAMETER [m]**	$v_{b,max}$**[m]**	T_b**[s]**	ξ_b**[%]**	**μ**	M_b**[t]**
1	FIP D 130-400	2.535	0.430	0.200	2.78	15.32	0.025	50
2	FIP D 400-600	3.725	0.655	0.300	3.38	15.08	0.025	250
3	NEW	0.850	0.350	0.150	1.73	8.00	0.025	30

Table 3. Properties of the Superstructure.

N°	**SUPERSTUCTURE**	**CROSS-SECTION [m]**	**HEIGHT [m]**	ξ_b**[%]**	**M [t]**
1	COLUMN	0.4	3	5.00	50
2	COLUMN	0.8	3	5.00	50
3	COLUMN	0.3	3	5.00	30

The analyses are performed for three different types of structures, which are defined as a function of the geometrical and mechanical characteristics of the isolator, of the masses of superstructure and substructure and of the stiffness of the superstructure (Table 2 and Table 3).

FIRST SERIES OF ANALYSES

The first series of analyses are performed by applying to the structures defined in Table 2 and Table 3 the ground motions listed in Table 1 and considering all the models described previously. Models A, B, C and D are applied to the structures subjected to the horizontal seismic component only, while model E is applied to the structures subjected to both horizontal and vertical seismic component. In these analyses, the selected ground motions are applied without any scaling factor. In this case it is necessary to calculate a proper value of the displacement $v_{b,max}$ for the analytical model A. To solve this problem we adopt an iterative procedure that allows to obtain a more accurate calculation of the maximum displacement $v_{b,max}$ through the elastic displacement spectrum. Thanks to Eq.(13) it is possible to correlate the period of the isolated structure with the maximum displacement, thus obtaining a curve (called periods curve) in the displacement-period plane (Fig.3).

$$T_b = 2\pi\sqrt{\frac{m+m_b}{k_b}} = 2\pi\sqrt{\frac{R\,v_{b,\max}}{\left(v_{b,\max}+\mu R\right)g}} \tag{13}$$

Each point of the periods curve is associated to a displacement value that in turns corresponds to a damping ratio according to the simplified Eq.(6). Each reduced elastic displacement spectrum, associated to a given damping, intersects the period curve in a certain point. The point to be considered is the one that is associated to the same damping in the periods curve and in the

displacement spectrum. Fig.3 shows the above procedure for El Centro record and the first system. The obtained values of damping and displacement are 21% and 0.131 m respectively.

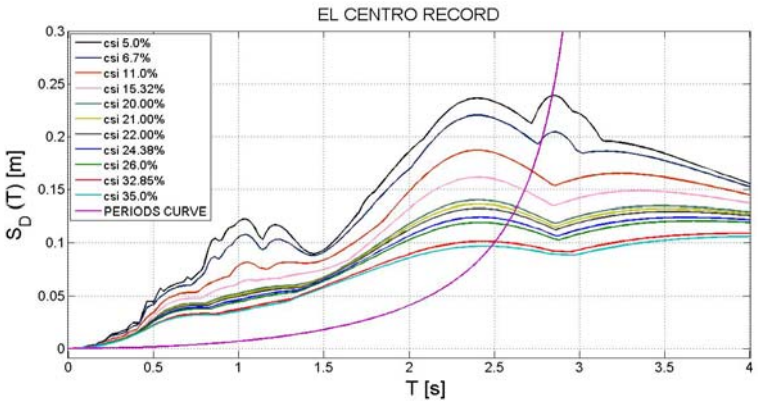

Figure 3. Reduced displacement spectra for El Centro record and periods curve for the selected isolator.

Thanks to this procedure, we can calculate the parameters of the elastic model A, so that the results can be compared with those of other models. Fig.4 and Fig.5 show the results obtained from the first series of analyses for the first system with the different models adopted for constant and variable normal force. Table 4 illustrates the results obtained from the analyses of the first system; the ground motions which cause traction in the isolators are highlighted. The results indicate that the models with constant friction coefficient, A and B, determine very similar results; this is due to the calibration procedure of $v_{b,max}$; on the contrary, models A and B, compared to those with variable friction coefficient, C and D, provide larger values of displacements and lower forces. Models C and D provide similar values of displacements and forces. Model E, with variable normal force, compared with models with constant normal force, C and D, provides values of displacements very similar but higher forces.

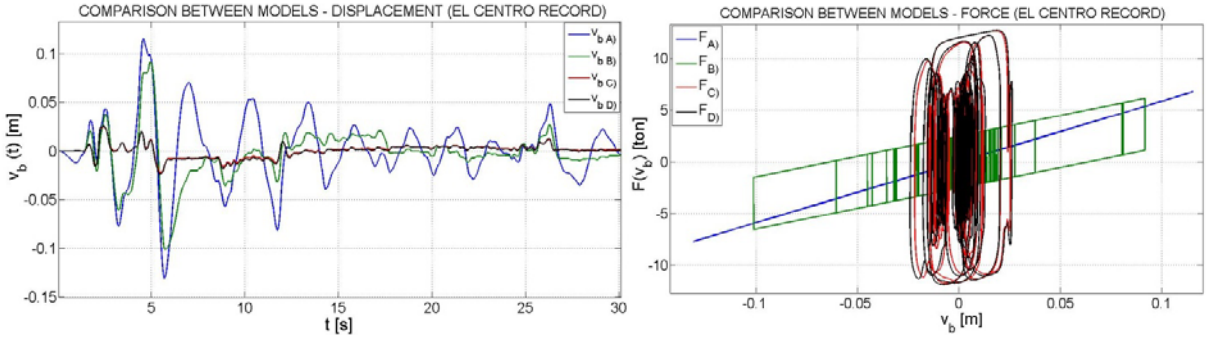

Figure 4. Results of models with constant normal force (El Centro record).

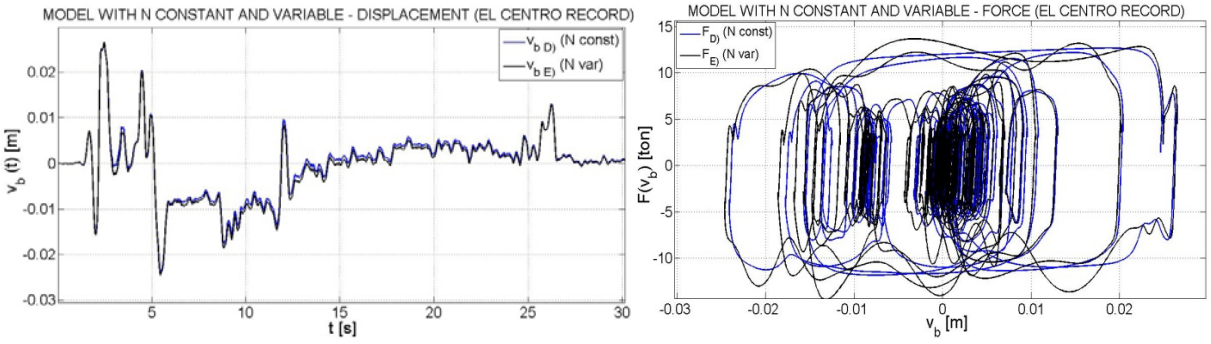

Figure 5. Results of models with constant and variable normal force (El Centro record).

Table 4. Values of displacements and forces obtained with all models for the first system.

Isolator FIP D 130-400 (R = 2535) $v_{b,max} = \pm 0.2$ m											
RECORD	**MAX DISPLACEMENT**					**MAX FORCE**					**ISOLATOR STATE**
	N CONST (H)				**N VAR (H+V)**	**N CONST (H)**				**N VAR (H+V)**	
	$v_{b\,A)}$ **[m]**	$v_{b\,B)}$ **[m]**	$v_{b\,C)}$ **[m]**	$v_{b\,D)}$ **[m]**	$v_{b\,E)}$ **[m]**	$F_{b\,A)}$ **[ton]**	$F_{b\,B)}$ **[ton]**	$F_{b\,C)}$ **[ton]**	$F_{b\,D)}$ **[ton]**	$F_{b\,E)}$ **[ton]**	**TRACTION**
1	-0.1310	0.1013	0.025	0.026	0.027	-7.66	-6.50	12.62	12.67	14.44	NO
2	-0.4498	-0.4324	-0.2820	-0.2840	-0.2894	-19.8	-19.5	-22.9	-22.96	-32.3	YES
3	0.3741	-0.404	0.2052	0.2104	0.2166	17.2	-18.4	19.7	20	28.3	NO
4	-0.0197	0.0302	-0.0069	-0.0077	-0.0077	-3.2	3.7	-9.3	-9.7	-9.9	NO
5	-0.3150	-0.3180	0.1382	0.1395	0.1378	-14.9	-15.0	17.0	17.1	24.6	NO
6	0.1054	0.1130	-0.0510	-0.0546	-0.0593	6.6	7.0	-13.5	-13.6	-19.3	NO
7	0.7059	0.6144	0.0716	0.0717	0.0707	30.3	26.7	14.3	14.3	16.5	NO
8	-0.0381	0.0364	-0.0143	-0.0157	-0.0168	-4.0	3.9	-11.7	-11.7	15.5	NO
9	0.2925	0.2755	0.0936	0.0974	0.1002	14.01	13.37	15.09	15.24	18.91	YES

For the models with constant friction coefficient (A and B) it would be necessary to investigate the constant friction coefficient (in order to obtain comparable results in terms of displacement). We can see from Table 5 that the constant friction coefficient that allows to obtain this result, for the first system, tends to be close to 0.12, which is the value of the maximum friction coefficient f_{max} obtained by linear interpolation of the experimental results, as suggested by Constantinou et al. (1991) for high sliding velocity. The study on the calculation of the right friction coefficient to be used in the comparison of the various analyses reveals a recurring problem in the use of constant friction models, which is the excessive sticking that we find in the time history of the displacement of the degree of freedom related to the isolation system. In Fig.6 we can see the differences in terms of displacement in the time history and force-displacement cycles for models B and D with constant normal force for the first system (with modified friction coefficient for model B).

Table 5. Values of constant friction coefficients for models A and B (first system).

Accel.	**ELCE**	**PACO**	**NEWH**	**SATI**	**KJM**	**COPP**	**STURN**	**TOL**	**MIRA**
μ	0.11	0.115	0.13	0.114	0.11	0.095	0.11	0.125	0.12

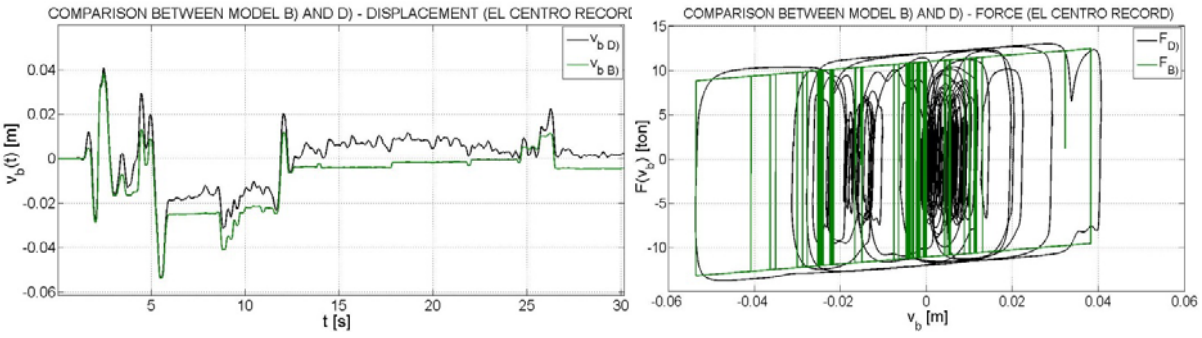

Figure 6. Comparison between models B and D with modified friction coefficient (first system).

SECOND SERIES OF ANALYSES

The purpose of these analyses is to study the response of the selected systems by considering similar intensities for the ground motions. Starting from the values of maximum displacement, period and damping (Table 2) for each type of isolator, we try to find the scale factor that will lead to the same maximum displacement as the one of the equivalent elastic model A. In order to calculate the scale factor it is necessary to consider the elastic displacement spectrum associated to the isolation damping.

For the period of the isolation system, we find the relative ordinate of the spectrum. This ordinate is the displacement value used to calculate the scale factor.

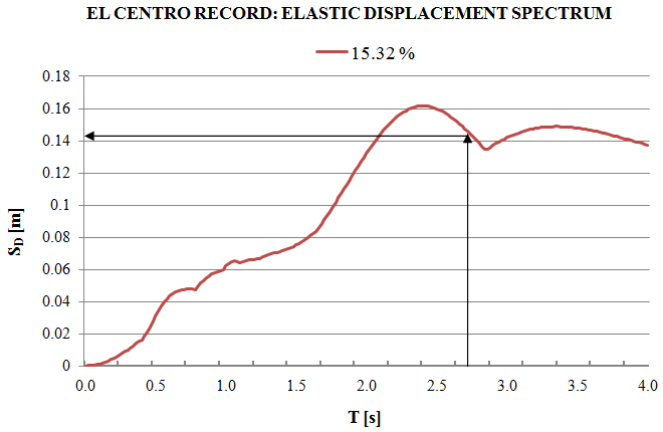

Figure 7. Elastic displacement spectrum for the El Centro record relative to the damping ratio of the FIP D 130-400 (2535) isolator.

For the FIP D 130-400 (2535) isolator, which is characterized by a damping ratio equal to 15.32% and by a period equal to T_b = 2.78 s, a displacement $S_D(T_b)$ = 0.1403 m is obtained for the El Centro record (Fig.7). The scale factor is:

$$f_{scale} = \frac{v_{b,\max}}{S_D(T_b)} = \frac{0.2}{0.1403} = 1.4255 \tag{14}$$

The scale factor obtained with this procedure may be not conservative if the analyses, conducted with the model E, indicate the presence of traction in the isolator. In this case it is necessary to calibrate the scale factor with an iterative procedure (underlined values in Table 6).

Table 6. Values of the scale factors of the accelerograms for the following analyses of the three considered systems.

	FIP D 130-400 (R = 2535) $v_{b,max}$ = 0.2 m T_b = 2.78 s		**FIP D 400-600 (R = 3725) $v_{b,max}$ = 0.3 m T_b = 3.38 s**		**NEW D = 300 (R = 850) $v_{b,max}$ = 0.15 m T_b = 1.73 s**	
RECORD	**$S_D(T_b)$ [m]**	**Scale Factor**	**$S_D(T_b)$ [m]**	**Scale Factor**	**$S_D(T_b)$ [m]**	**Scale Factor**
ELCE	0.1403	1.38 (1.4255)	0.1495	2.0066	0.1197	1.2531
PACO	0.3880	0.5155	0.4157	0.61 (0.7217)	0.4380	0.3425
NEWH	0.3371	0.5934	0.3601	0.71 (0.8331)	0.3447	0.4352
SATI	0.0839	2.3840	0.0753	3.9841	0.0690	2.1739
KJM	0.2748	0.7278	0.2923	1.0263	0.3612	0.4153
COPP	0.1145	1.04 (1.7463)	0.1087	1.86 (2.7599)	0.1107	1.00 (1.3550)
STURN	0.4248	0.4708	0.4856	0.6178	0.1704	0.8803
TOLM	0.0545	1.52 (3.6690)	0.0583	1.32 (5.1458)	0.0641	2.15 (2.3401)
MIRA	0.2693	0.44 (0.7427)	0.2492	0.83 (1.204)	0.2555	0.45 (0.587)

The table below shows all the values of displacement and force that come from the different analyses with the different ground motions, both for constant and variable normal force in terms of mean, standard deviation and coefficient of variation (Table 7). The trend of the results is similar to the one described previously for the first series of analyses. Fig. 8 and Fig. 9 show the results obtained from the second series of analyses for the first system with the different models adopted for constant and variable normal force.

Table 7. Values of displacements and forces obtained with all models for the three systems in terms of mean ($\overline{\mu}$), standard deviation (σ) and coefficient of variation ($\sigma/\overline{\mu}$).

SYSTEM		MAX DISPLACEMENT					MAX FORCE				
		N CONST (H)				N VAR (H+V)	N CONST (H)				N VAR (H+V)
	STAT	$v_{b\,A)}$ [m]	$v_{b\,B)}$ [m]	$v_{b\,C)}$ [m]	$v_{b\,D)}$ [m]	$v_{b\,E)}$ [m]	$F_{b\,A)}$ [ton]	$F_{b\,B)}$ [ton]	$F_{b\,C)}$ [ton]	$F_{b\,D)}$ [ton]	$F_{b\,E)}$ [ton]
1	$\overline{\mu}$	0.1998	0.1773	0.0621	0.0640	0.0653	10.42	9.52	13.55	13.62	16.77
	σ	0.0006	0.0353	0.0394	0.0396	0.0403	0.0595	1.1151	1.9992	2.0127	3.8043
	$\sigma/\overline{\mu}$	0.0031	0.1990	0.6349	0.6183	0.6168	0.0057	0.1172	0.1475	0.1478	0.2269
2	$\overline{\mu}$	0.3	0.2843	0.0966	0.0983	0.0961	31.67	30.40	39.05	39.25	44.98
	σ	0	0.0296	0.0586	0.0585	0.0575	0.05	2.3846	6.6103	6.4542	11.726
	$\sigma/\overline{\mu}$	0	0.1043	0.6071	0.5956	0.5986	0.002	0.0784	0.1693	0.1644	0.2607
3	$\overline{\mu}$	0.1512	0.133	0.0463	0.0469	0.0488	12.183	10.900	9.433	9.433	10.900
	σ	0.0033	0.0201	0.0142	0.0139	0.0140	0.2858	1.4269	1.3633	1.1708	1.6432
	$\sigma/\overline{\mu}$	0.0217	0.1511	0.3054	0.2958	0.2877	0.0235	0.1309	0.1445	0.1241	0.1507

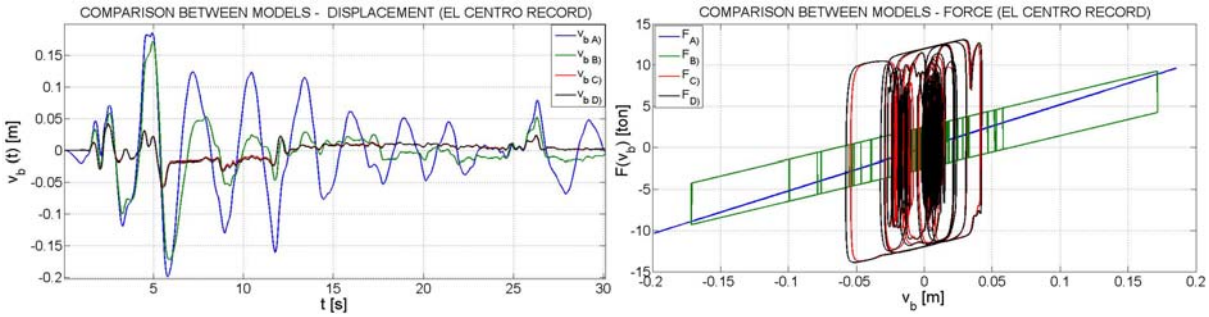

Figure 8. Results of models with constant normal force (El Centro record).

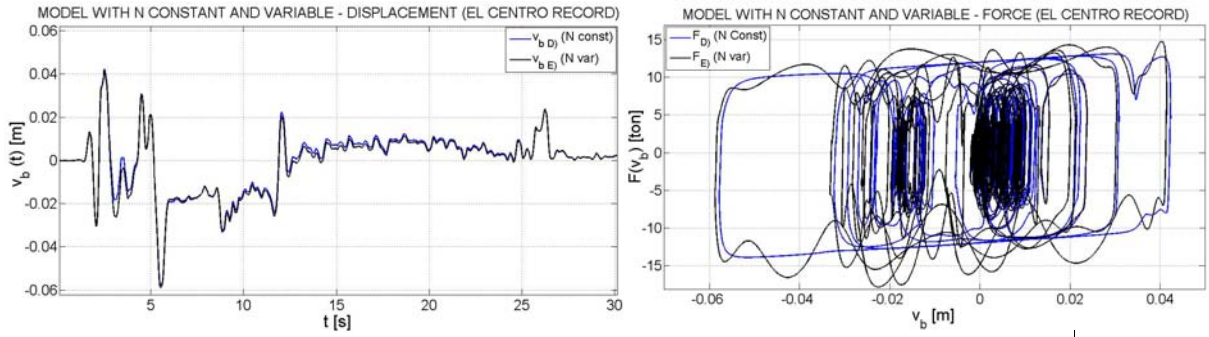

Figure 9. Results of models with constant and variable normal force (El Centro record).

DETERMINATION OF HORIZONTAL AND VERTICAL COLLAPSE FACTORS

The object of this paragraph is the study of the response for increasing values of the seismic intensity, for both horizontal and vertical ground motions. In general only the horizontal component is considered. However it may be not conservative. This study is aimed at finding horizontal and vertical amplification factors of the ground motions, in order to understand which is the acceleration that causes the collapse of the system. Firstly, the analyses are conducted with constant normal force in order to find the amplification factors of the horizontal seismic component that leads to the collapse displacement of the isolator (2nd and 3rd column of Table 8).

Table 8. Collapse factors with horizontal and vertical peak accelerations for the first system.

FIP D 130-400 (R = 2535) Isolator						
REC.	**HOR. COLLAPSE FACTOR**	PGA_H **[m/s^2]**	**VERT. COLLAPSE FACTOR**	PGA_V **[m/s^2]**	PGA_H **[m/s^2] VERT. COLLAPSE**	PGA_H **[m/s^2] COMBINED COLLAPSE**
1	2.80	8.60	1.38	2.77	4.24	4.24
2	0.83	9.98	0.71	4.86	8.53	8.53
3	0.97 (0.98)	5.62 (5.70)	1.07	6.22	6.22	5.62
4	6.25 (6.40)	7.69 (7.88)	12.70	6.41	15.60	7.69
5	1.35 (1.30)	10.89 (10.49)	1.55	5.23	12.50	10.89
6	2.30	14.9	1.04	5.06	6.73	6.73
7	1.52 (1.51)	5.34 (5.30)	2.10	5.36	7.36	5.34
8	5.15	17.77	1.52	3.99	5.24	5.24
9	1.38	3.98	0.44	3.84	1.27	1.27
$\overline{\mu}$	**-**	**9.42**	**-**	**4.86**	**7.52**	**6.17**

In these analyses, model D is used as more representative of the real behaviour of the FPS isolator. Secondly, the analyses in the vertical direction are conducted in order to find the amplification factor of the vertical seismic component that leads to the formation of traction in the isolator (4th and 5th columns of Table 8). The maximum horizontal ground acceleration associated to this amplification of the vertical component is then evaluated (6th column of Table 8). Finally the determined amplification factors and the corresponding collapse ground accelerations are compared. If the value of horizontal collapse acceleration, obtained without considering the vertical seismic component, is lower than the horizontal collapse acceleration obtained considering the vertical seismic component, then it is necessary to analyze the system with model E, which includes the influence of the variation of the normal force (the values out of brackets in the 3rd column of Table 8 are obtained with model E, while the values in brackets are obtained with model D). On the contrary, if the value of horizontal collapse acceleration, obtained considering only the vertical seismic component, is lower than the horizontal collapse acceleration obtained without considering the vertical seismic component, the collapse scale factor is the one associated to the vertical component. Table 8 shows the results for the first system. The 7th column shows the minimum between the values of horizontal collapse acceleration of 3rd and 6th columns. We can see that, if only the horizontal seismic component is considered and the collapse for traction is neglected, an overestimation of the maximum acceleration bearable by the isolator may be obtained. Considering the first system and the records 1, 6, 8 and 9, the collapse acceleration obtained neglecting the vertical seismic component is more than two times larger than the one obtained considering the vertical component. For the same system, the average value of the overestimation over all records is equal about to 1.25.

CONCLUSIONS

In this paper the influence of the modelling of the isolator seismic response on the global response of the structure has been studied through a comparison among different models. The analyses have been performed considering a set of ground motions with near field records characterized by different values of the ratio between the peak vertical and horizontal accelerations. The records have been also applied considering increasing values of intensity. The results have shown that a correct evaluation of the response requires to consider a model that account for the variation of the friction in the isolator with velocity and normal force. The models based on constant friction have provided results similar to those with variable friction when a value close to the maximum friction coefficient has been adopted. The results have highlighted also the importance of developing a design procedure that can take into account the influence of the vertical seismic component. In this way it is possible to avoid an overestimation of the maximum acceleration bearable by the isolation devices. Neglecting the vertical component has determined, in some cases, values of collapse acceleration also two times larger than considering the vertical component.

REFERENCES

Constantinou MC, Mokha A, Reinhorn A (1990) "Teflon bearings in base isolation. I: testing", *Journal of Structural Engineering*, 116(1), 435-455

Constantinou M C, Mokha A, Reinhorn A (1990) "Teflon bearings in base isolation. II: modelling" , *Journal of Structural Engineering*, 116(2), 455-474

Constantinou MC, Mokha A, Reinhorn A (1991) " Experimental study of friction-pendulum isolation system, *Journal of Structural Engineering*, 117, 1201-1217

Calvi GM, Ceresa P, Casarotti C, Bolognini D, Auricchio F (2004), "Effects of axial force variation in the seismic response of bridges isolated with fiction pendulum systems", *Journal of Earthquake Engineering*, 8(1), 187-224

Davis T, Mostaghel N (1997), "Representations of Coulomb friction for dynamic analysis", *Earthquake Engineering and Structural Dynamics*, 26, 541-548

Diotallevi PP, Landi L (2006), "Response of RC structures subjected to horizontal and vertical ground motions", *8th US National Conference on Earthquake Engineering* , San Francisco, 4113-4122

Diotallevi PP, Landi L, Benni S (2006), "Effect of near-fault ground motions on the response of base isolated structures", *8th US National Conference on Earthquake Engineering*, San Francisco, 4847-4856

Kelly JM, Naeim F (1999), Design of seismic isolated structures. From theory to practice, John Wiley & Sons, Inc.

Mazza F, Vulcano A (2008), "Effects of horizontal and vertical near-fault ground motions on the nonlinear dynamic response of RC buildings with different base-isolation systems", *14th WCEE*

Mosqueda G, Whittaker AS, Fenves GL (2004), "Characterization and modeling of friction pendulum bearings subjected to multiple components of excitation", *Journal of Structural Engineering*, 130(3), 433-442

Mostaghel N (2004),"A non-standard analysis approach to systems involving friction", *Journal of sound and vibration*, 284, 583–595

Papazoglou AJ, Elnashai AS (1996), "Analytical and field evidence of the damaging effect of vertical earthquake ground motion", *Earthquake Engineering and Structural Dynamics*, 25, 1109-1137

Wen YK (1976), "Method of random vibration of hysteretic system", *J. Eng. Mech. Div.,*102(2), 249-263

Zayas V, Low S, Mahin S (1987) "The FPS earthquake protection system: Experimental report" *, Earthquake Engineering Research Center*, Univ. of California, Berkeley, Report No UCB/EERC-87/01